

Turbulence in Class 0 and Class I protostellar envelopes

D. Ward-Thompson¹, L. Hartmann², D. J. Nutter¹

¹*Department of Physics and Astronomy, Cardiff University, PO Box 913, Cardiff, CF24 3YB*

²*Harvard-Smithsonian Center for Astrophysics, 60 Garden Street, Cambridge, MA02138, USA*

Accepted 2004 November 18; received 2004 November 17; in original form 2003 October 17.

ABSTRACT

We estimate the levels of turbulence in the envelopes of Class 0 and I protostars using a model based on measurements of the peak separation of double-peaked asymmetric line profiles. We use observations of 20 protostars of both Class 0 & I taken in the HCO^+ ($J=3\rightarrow 2$) line that show the classic double-peaked profile. We find that some Class 0 sources show high levels of turbulence whilst others demonstrate much lower levels. In Class I protostars we find predominantly low levels of turbulence. The observations are consistent with a scenario in which Class 0 protostars form in a variety of environments and subsequently evolve into Class I protostars. The data do not appear to be consistent with a recently proposed scenario in which Class 0 protostars can only form in extreme environments.

Key words: radiative transfer – stars: formation – ISM: clouds – submillimetre.

1 INTRODUCTION

A model for the evolution of the youngest protostars has emerged over the last decade or more, based on a great deal of observational evidence. In this model the protostar evolves through a series of recognisable stages in which a circumstellar envelope of material collapses onto a central protostar and its surrounding disc (see André, Ward-Thompson & Barsony 2000 for a review).

In this scenario the first recognisable stage of protostellar evolution is known as the Class 0 stage (André, Ward-Thompson & Barsony 1993 – hereafter AWB93), which is defined in such a way that the circumstellar envelope contains more mass than the central protostar. The next stage is known as the Class I stage (Lada & Wilking 1984; Lada 1987), in which there is still a massive envelope, although there is more mass in the central protostar. The subsequent Class II & III stages (Lada & Wilking 1984; Lada 1987) represent protostars whose circumstellar envelopes have been dissipated, but in which there is still a circumstellar disc (e.g. Kenyon & Hartmann 1995; Safier, McKee & Stahler 1997). The Class II & III stages are also known as the classical T Tauri (CTT) and weak-line T Tauri (WTT) stages respectively (André & Montmerle 1994).

Infall from the protostellar envelope onto the protostar can be inferred from the double-peaked asymmetric spectral line profiles of certain molecular species (e.g. Zhou 1992; 1995; Rawlings et al. 1992; Zhou et al. 1993; Ward-Thompson et al. 1996). There are a number of explanations for the manner in which the asymmetry arises, but the usually accepted explanation is based on the observer

preferentially seeing warmer blue-shifted material closer to the protostar and cooler red-shifted material further from the protostar (Zhou 1992). Infall profiles have now been observed towards many protostars (e.g. Gregersen et al. 1997; 2000).

Our understanding of the evolutionary process has been formalised into a luminosity versus colour diagram analogous to the HR diagram, using the bolometric luminosity of the protostar, L_{Bol} , and a ‘bolometric temperature’, T_{Bol} (Myers & Ladd 1993). The bolometric temperature is based on the position of the peak wavelength of the continuum emission from the protostar. The more evolved the protostar, the greater its measured value of T_{Bol} . Hence T_{Bol} provides a useful evolutionary ‘age’ indicator for protostars.

Recent work based on chemical modelling of protostellar envelopes appears to support the idea that Class I sources are more evolved than Class 0 sources (Buckle & Fuller 2003). These authors modelled the chemical evolution of sulphur-bearing molecules and showed that Class I protostellar envelopes are more chemically evolved in general than the envelopes of Class 0 protostars.

However, the role of turbulence in the star formation process is still a matter for debate (e.g. Elmegreen 2002). In this paper we endeavour to measure the relative amounts of turbulence in Class 0 & I protostellar envelopes by measuring the peak separation in a sample of protostars. Furthermore, we interpret the variation in separations observed in terms of our recent radiative transfer model results. In this model the velocity separation of the peaks is seen to be dominated by the relative level of turbulence in the infalling protostellar envelope.

arXiv:astro-ph/0412219v1 9 Dec 2004

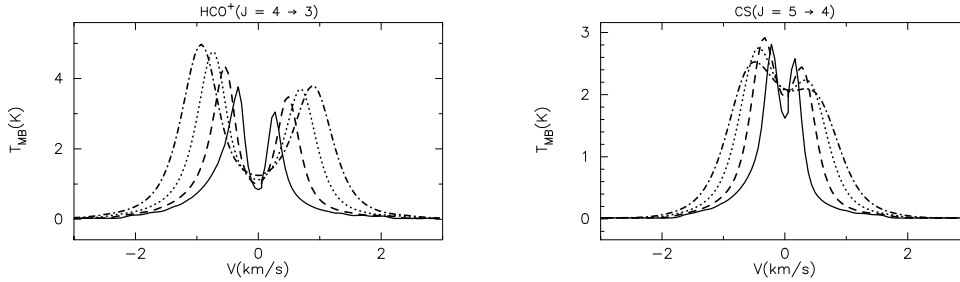


Figure 1. Plots showing the dependence of the predicted $\text{HCO}^+(\text{J}=4 \rightarrow 3)$ and $\text{CS}(\text{J}=5 \rightarrow 4)$ line profiles on the magnitude of the turbulent velocity dispersion in the protostellar envelope (assumed to be constant throughout the envelope). Spectra are plotted for turbulent velocity dispersions of 0.1 km/s (solid lines), 0.2 km/s (dashed lines), 0.3 km/s (dotted lines) and 0.4 km/s (dot-dashed lines). The equivalent FWHM turbulent velocity widths are found by multiplying these numbers by 2.35. Note that increasing turbulence increases the peak separation. The same effect is also seen in other transitions, such as $\text{HCO}^+(\text{J}=3 \rightarrow 2)$.

2 MEASURING TURBULENCE

The presence of non-thermal motions in molecular cloud regions where stars are formed has been recognised for some time (e.g. Caselli & Myers 1995). These non-thermal motions are usually attributed to the presence of turbulence (e.g. Padoan & Nordlund 2002). Measuring the exact levels of turbulence in molecular clouds can be complicated. However, the fact that turbulence plays a significant role in the star formation process is now widely recognised (e.g. Elmegreen 2002 and references therein).

We have recently carried out detailed spectral modelling of protostellar infall candidates (Ward-Thompson & Buckley 2001). This process uses a radiative transfer Λ -iteration model based on the method of Stenholm (1977). The method was refined by subsequent workers (Matthews 1986; Heaton et al. 1993; Buckley 1997). It solves the spectral line radiative transfer problem for the rotational transitions of linear molecules in a spherically symmetric model cloud. The radial profiles of infall velocity, temperature, density, tracer molecule abundance and micro-turbulent velocity dispersion may be specified (Ward-Thompson & Buckley 2001).

The method is begun by choosing an initial radiation field in a more or less arbitrary manner. From this, a ‘false’ set of molecular energy level populations are calculated. Radiative transitions between these populations will generally produce a radiation field which departs from the initial field. If this radiation field is used to calculate a new set of populations, and the procedure is repeated a sufficiently large number of times, the radiation field and populations should eventually converge on a mutually consistent solution (for further details see Ward-Thompson & Buckley 2001). The output spectra are convolved with a chosen beam size to match any given set of observations. We have applied the method to HCO^+ and CS spectral line observations of protostellar envelopes and modelled their infall parameters.

Figure 1 shows the predicted line profiles that would be observed at the James Clerk Maxwell Telescope (JCMT) in the $\text{HCO}^+(\text{J}=4 \rightarrow 3)$ and $\text{CS}(\text{J}=5 \rightarrow 4)$ molecular line transitions to match some of the data we show below. The beam convolution to match the Caltech Submillimeter Observatory (CSO) data also shown below does not significantly alter the results. The model assumes an inside-out collapse in which an expansion wave has reached a radius that we call the infall radius, outside of which the velocity is zero.

We assume that a mass $M_{\odot}/2$ has already accreted onto the central protostar, and a further $M_{\odot}/2$ of envelope gas is infalling towards it. We choose an effective sound speed of $a_{\text{eff}} = 0.35 \text{ km s}^{-1}$. We use model relations for the radial velocity and density profiles consistent with the inside-out collapse scenario of $\rho \propto r^{-3/2}$ inside the infall radius and $\rho \propto r^{-2}$ outside the infall radius. We truncate the density profile at an outer radius of 10000 AU, which encloses a total mass of $2.75 M_{\odot}$. The temperature profile in the optically thin part of the envelope is chosen to have a canonical profile $T \propto r^{-0.4}$. The parameter normalisations used in the radiative transfer modelling are given by Ward-Thompson & Buckley (2001) and the molecular constants are taken from the catalogue of Poynter & Pickett (1985).

Figure 1 shows how the line profiles depend on the magnitude of the turbulent velocity dispersion, σ_{tb} , when it is assumed to be uniform throughout the envelope. As the turbulent velocity dispersion increases, the most apparent effect on the line profile is to increase the velocity separation between the two peaks. Figure 1 shows the results for $\text{HCO}^+(\text{J}=4 \rightarrow 3)$, and $\text{CS}(\text{J}=5 \rightarrow 4)$. A similar result is also seen in the $\text{HCO}^+(\text{J}=3 \rightarrow 2)$ transition.

The magnitude of the change in the line-shape observed in Figure 1 is totally different to that caused by increasing the optical depth. Myers et al. (1996) explored the manner in which increasing the optical depth changed the line-shape (see their figure 2a). They plotted the two extremes of optical depth that can cause a double-peaked profile to be observed, and found that they produced an increase of peak separation of only $\leq 0.1 \text{ km s}^{-1}$. Likewise, we find from our model that an increase of ~ 2 in optical depth results in an increase of peak separation of only $\sim 0.2 \text{ km s}^{-1}$ (c.f. figures 12 and 13 of Ward-Thompson & Buckley 2001). These two numbers can be compared to the differences of order ~ 1 – 2 km s^{-1} caused by increasing turbulence, as seen in Figure 1. Thus it can be seen that variations in optical depth will only introduce a small scatter in the observed peak separation, which is dominated by variations in levels of turbulence.

Hence we see that the relative level of turbulence in protostellar envelopes can be estimated from the relative separation of the two peaks of the classic double-peaked asymmetric infall profile. No other parameter has such a large effect on the separation of the two peaks (Ward-Thompson & Buckley 2001). Even though the profiles in Figure 1 are

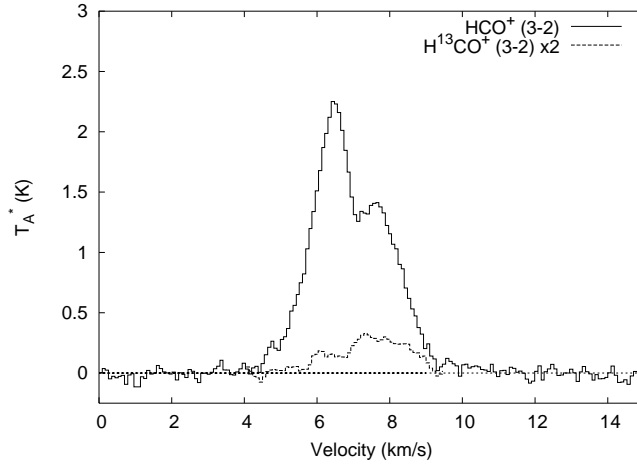


Figure 2. $\text{HCO}^+(\text{J}=3\rightarrow 2)$ spectrum of L1489 showing the double-peaked asymmetric line profile (solid line). Also shown is the $\text{H}^{13}\text{CO}^+(\text{J}=3\rightarrow 2)$ isotope line (dashed line), multiplied by 2, illustrating that the optically thin isotope is single-peaked.

Table 1. Summary of all of the data used in our analysis, listed in order of increasing bolometric temperature. Column 1 lists the usual source name, column 2 lists the bolometric temperature, T_{Bol} , column 3 indicates whether it is a Class 0 or I protostar, column 4 gives the separation between the two peaks of the asymmetric line profile (see text for details). Column 5 contains the following notes: (1) Our data; (2) data taken from Gregersen et al. (1997); (3) data taken from Gregersen et al. (2000).

| Name | T_{Bol} (K) | Class | Separation (km/s) | Notes |
|----------------|-------------------------|-------|----------------------|-------|
| B335 | 29 | 0 | 0.78 | 2 |
| NGC1333 IRAS4A | 34 | 0 | 1.70 | 2 |
| Serpens SMM4 | 35 | 0 | 2.17 | 2 |
| NGC1333 IRAS4B | 36 | 0 | 1.53 | 2 |
| Serpens SMM2 | 38 | 0 | 1.23 | 2 |
| L1527 | 41 | 0 | 0.85 | 2 |
| L1157 | 44 | 0 | 0.97 | 2 |
| Serpens SMM1 | 45 | 0 | 2.48 | 2 |
| B228 | 48 | 0 | 0.55 | 3 |
| NGC1333 IRAS2 | 52 | 0 | 1.57 | 3 |
| L1448N | 55 | 0 | 0.90 | 1 |
| CB244 | 56 | 0 | 0.87 | 3 |
| IRAS 23011 | 57 | 0 | 1.01 | 3 |
| IRAS 20050 | 69 | 0 | 2.03 | 2 |
| L1634 | 77 | I | 0.71 | 3 |
| IRAS 04166 | 91 | I | 0.72 | 3 |
| L1251B | 91 | I | 1.36 | 3 |
| IRAS 03235 | 136 | I | 0.73 | 3 |
| TMC 1A | 170 | I | 0.61 | 3 |
| L1489 | 238 | I | 1.10 | 1 |

calculated for the specific parameters listed above, the same effect of increasing peak separation with increasing turbulence was seen in all models. We now use this diagnostic to estimate the relative levels of turbulence in the envelopes of protostars.

3 DATA

The majority of the data we use are taken from the literature, but data for two additional sources were obtained. L1489 was observed at a position of R.A. (1950) = $04^{\text{h}} 01^{\text{m}} 40.6^{\text{s}}$, Dec. (1950) = $+26^{\circ} 10' 49''$ and L1448N was observed at a position of R.A. (1950) = $03^{\text{h}} 22^{\text{m}} 31.8^{\text{s}}$, Dec. (1950) = $+30^{\circ} 34' 45''$. These observations were carried out at the James Clerk Maxwell Telescope (JCMT) on 2001 August 10, using the receiver RxA2 (Davies et al. 1992), with the Digital Autocorrelation Spectrometer (DAS) backend. The DAS was configured with the optimum frequency resolution of 95kHz per channel, equivalent to $\sim 0.1 \text{ km s}^{-1}$. This is very similar to the resolution of the literature data that we use. The observations were made using frequency switching mode (Matthews 1996). All data reduction was carried out using the SPECX package (Padman 1990).

Figure 2 shows a typical result for one of the $\text{HCO}^+(\text{J}=3\rightarrow 2)$ spectra. We see the two peaks of the line profile, separated by an absorption dip, and the characteristic infall asymmetric profile. From such a spectrum the positions of the red and blue peaks can be obtained to an accuracy of roughly one spectral channel, or $\sim 0.1 \text{ km s}^{-1}$.

We have spectral line data for a total of 20 sources – 14 Class 0 protostars and 6 Class I protostars – in transitions of $\text{HCO}^+(\text{J}=3\rightarrow 2)$ and $\text{H}^{13}\text{CO}^+(\text{J}=3\rightarrow 2)$. It is necessary to obtain data in the optically thin isotope line to check that the two peaks being observed in the main isotope line are not due to two different clouds along the same line of sight. We could confirm that the rare isotope line was single-peaked in each case. The data are listed in Table 1. All 20 sources have been well studied previously, and have known continuum spectra and bolometric temperatures. Table 1 lists the source name, its bolometric temperature and Class. Table 1 also lists the measured peak separation of the double-peaked spectra and the source of the literature data.

4 DISCUSSION AND CONCLUSIONS

Figure 3 shows a plot of peak separation versus T_{Bol} for the sources listed in Table 1. As shown above, peak separation scales with turbulence level. Consequently those sources

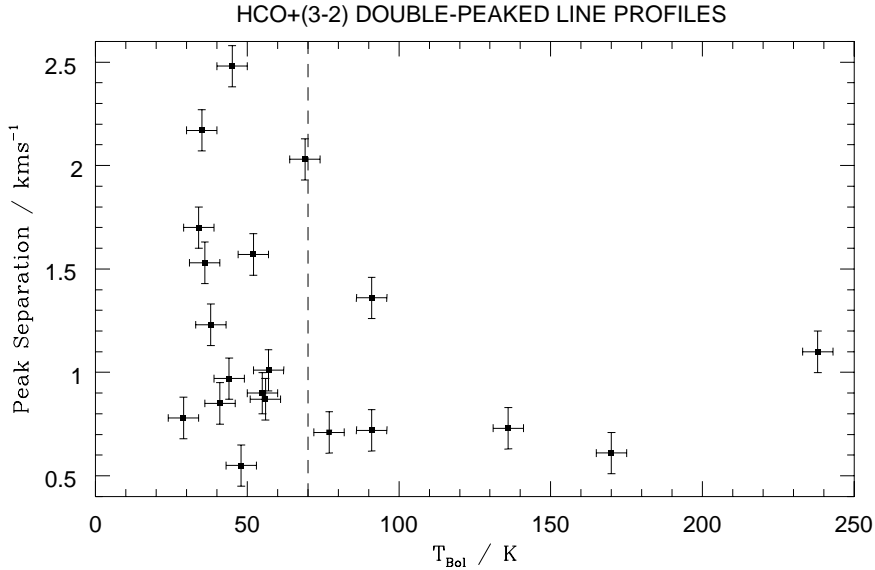


Figure 3. Graph of peak separation versus T_{Bol} for Class 0 & I protostars. Large peak separations are equivalent to high levels of turbulence. Higher values of T_{Bol} correspond to more evolved protostars in the evolutionary scenario. The vertical dashed line represents the border between Class 0 and Class I. Note that there are both high and low levels of turbulence observed in Class 0 protostars.

showing high levels of turbulence appear in the upper parts of the graph, while those with lower levels of turbulence appear in the lower parts of the graph. The error-bars correspond to $\pm 5\text{K}$ and $\pm 0.1\text{kms}^{-1}$. T_{Bol} is used simply as a way of separating the Class 0 protostars from the Class I protostars. The definition of a Class 0 protostar corresponds to it having $T_{\text{Bol}} < 70\text{K}$. The vertical dashed line is the dividing line between Class 0 and I protostars.

In Figure 3 we see Class 0 protostars with a wide variety of levels of turbulence in their envelopes, although we see that there are predominantly low levels of turbulence in Class I sources. Figure 3 is consistent with the evolutionary scenario proposed by AWB93, in which Class 0 sources can form in regions of both high and low turbulence, before evolving into Class I protostars.

One interesting facet of the data is that there do not appear to be any Class I protostars in Figure 3 with high turbulence levels. This may not be statistically significant, due to the smaller number of Class I sources. However, if future data prove that this is also significant, then this appears to be saying that any initial turbulence in the environment of a forming protostar dissipates before it has evolved to the Class I stage. The more massive envelopes in the earlier Class 0 protostars can sustain relatively high initial levels of turbulence when they occur. However, by the Class I stage when more than half of the envelope has accreted onto the central protostar, a large percentage of any initial turbulence has been dissipated.

We independently estimated the line optical depths for the data in Table 1 (using the isotope line data), and confirmed that they lie in the range $\sim 1.5\text{--}3.5$, consistent with the regime of parameters that we are modelling (see discussion in section 2 above). We plotted optical depth versus peak separation and found no correlation. This appears to confirm our assertion that the peak separation is not dominated by optical depth effects, but rather by turbulence.

We note finally that an alternative evolutionary sce-

nario for the Class 0 & I protostellar stages has recently been proposed (Jayawardhana, Hartmann & Calvet, 2001 – hereafter JHC) in which Class 0 protostars only form in high density environments whilst Class I protostars form in low density environments, and the two stages are in fact parallel evolutionary tracks. In this scenario the high density environments required to produce Class 0 protostars are produced by invoking colliding turbulent flows (see discussion in section 4.3 of JHC). Under such a scenario one might expect that this additional turbulence required to produce Class 0 protostars would be measurable, and that all Class 0 sources should exhibit high levels of turbulence. Figure 3 shows this not to be the case, and therefore appears to be inconsistent with the JHC scenario.

ACKNOWLEDGMENTS

The authors would like to thank the staff of the JCMT for assistance while these data were obtained. JCMT is operated by the Joint Astronomy Centre, Hawaii, on behalf of the UK PPARC, the Netherlands NWO, and the Canadian NRC. DJN acknowledges PPARC for PDRA support.

REFERENCES

- André P., Montmerle T., 1994, *ApJ*, 420, 837
- André P., Ward-Thompson D., Barsony M., 1993, 406, 122 (AWB93)
- André P., Ward-Thompson D., Barsony M., 2000, in: Mannings V., Boss A. P., Russell S. S., eds., ‘Protostars & Planets IV’, 59, University of Arizona Press, Tucson
- Buckle J. V., Fuller G. A., 2003, *A&A*, 399, 567
- Buckley H. D., 1997, PhD Thesis, University of Edinburgh
- Caselli P., Myers P. C., 1995, *ApJ*, 446, 665
- Davies S. R., Cunningham C. T., Little L. T., Matheson D. N., 1992, *Int. J. Infrared Millimetre Waves*, 13, 647
- Elmegreen B. G., 2002, *ApJ*, 577, 206

- Gregersen E. M., Evans N. J. II, Mardones D., Myers P. C., 2000, ApJ, 533, 440
- Gregersen E. M., Evans N. J. II, Zhou S., Choi M., 1997, ApJ, 484, 256
- Heaton B. D., Little L. T., Yamashita T., Davies S. R., Cunningham C. T., Monteiro T. S., 1993, A&A, 278, 238
- Jayawardhana R., Hartmann L., Calvet N., 2001, ApJ, 548, 310 (JHC)
- Kenyon S. J., Hartmann L. W., 1995, ApJSS, 101, 117
- Lada C. J., 1987, in: Peimbert M., Jugaku J., eds., 'Star Forming Regions', IAU Symposium 115, 1, Reidel, Dordrecht
- Lada C. J., Wilking B., 1984, ApJ, 287, 610
- Matthews H., 1996, 'JCMT Guide for Prospective Users', JAC, Hawaii
- Matthews N., 1986, PhD Thesis, University of Kent
- Myers P. C., Ladd E. F., 1993, ApJ, 413, L47
- Myers P. C., Mardones D., Tafalla M., Williams J. P., Wilner D. J., 1996, ApJ, 465, L133
- Padman R., 1990, 'Specx Users Manual', Cavendish Laboratory, University of Cambridge
- Padoan P., Nordlund A., 2002, ApJ, 576, 870
- Poynter R. L. Pickett H. M., 1985, Applied Optics, 24, 2235
- Rawlings J. M. C., Hartquist T. W., Menten K. M., Williams D. A., MNRAS, 1992, 255, 471
- Safier P. N., McKee C. F., Stahler S. W., 1997, ApJ, 485, 660
- Stenholm L. G., 1977, A&A, 54, 577
- Ward-Thompson D., Buckley H. D., 2001, MNRAS, 327, 955
- Ward-Thompson D., Buckley H. D., Greaves J. S., Holland W. S., André P., 1996, MNRAS, 281, L53
- Zhou S., 1992, ApJ, 394, 204
- Zhou S., 1995, ApJ, 442, 685
- Zhou S., Evans N. J., Kompe C., Walmsley C. M., 1993, ApJ, 404, 232